

600 SCC Ce

## The effect of alloying Ce on the SCC behavior of Alloy 600

150

[600CE4 (Ni-15Cr-9Fe-0.03C-0.04Ce) 600CE0 (Ni-15Cr-9Fe-0.03C)]  
 600 (SCC) Ce 가  
 TEM EDX Cr Cr Cr<sub>7</sub>C<sub>3</sub> 가 SEM  
 Cr Cr Ce 가 SCC . Ce가 가  
 SCC 가 .

. TT .  
 . 315 40% NaOH .

## Abstract

High purity model alloys with major composition Ni-15Cr-9Fe-0.03C (600CE0) and Ni-15Cr-9Fe-0.03C-0.04Ce (600CE4) were produced. Using these model alloys the effect of alloying Ce on the SCC behavior of Alloy 600 was evaluated. To obtain carbides precipitated on grain boundaries, the thermal treatment was performed on both the solution annealed alloys. Microstructural examinations using SEM and TEM EDX showed that the same structural carbides, Cr<sub>7</sub>C<sub>3</sub>, were precipitated on both the alloys and no significant difference in the amount of Cr depletion along grain boundaries was observed between the two model alloys. However, it was shown that the coverage of grain boundary carbides was higher in the Ce-bearing alloy (600CE4). The SCC susceptibility of the alloys was investigated in 40%NaOH solution at 315°C. Being evaluated in terms of maximum crack depth, the SCC susceptibility of the alloy turned out to be reduced by the addition of Ce. The increased resistance to the SCC in the alloy 600CE4 was considered to be attributable to the increased coverage of grain boundary carbides.

# 1.

Ni 600 가 Ni-16Cr-9Fe , 가 , , 가 (Pitting), (Denting), (Intergranular Attack, IGA), (Stress Corrosion Cracking, SCC) (Intergranular Stress Corrosion Cracking, IGSCC) 가 1 (Primary Water Intergranular Stress Corrosion Cracking) 2 (tube sheet) (tube support plate) 2 [1]. 가 , 600 SCC 가 [2,3] 2 TiO<sub>2</sub>, TiB<sub>2</sub>, CeB<sub>6</sub>, LaB<sub>6</sub> 가[4] . Alloy 600 Ce 가 Ce가 Alloy 600 SCC

# 2.

## 2.1

Ni-15Cr-9Fe Ce 가 (600CE0) , Ce 가 (600CE4) 30kg ingot , 1250 135 , 7mm H<sub>2</sub>O:HNO<sub>3</sub>:HCl:H<sub>2</sub>O<sub>2</sub> 3:2:2:1 , 1.5mm 1 .

Table 1 Chemical compositions of the alloys used in this study (wt.%)

	C	Ni	Cr	Fe	Ce
600CE0	0.03	75.25	15.24	9.28	0.003
600CE4	0.03	74.66	15.41	9.72	0.04

## 2.2

(solution annealing, SA) 900~1100 . Alloy 600 SCC  
 가 TT  
 [3]. 704 2~96  
 DC 4.5V 30 , nital  
 bromine (bromine+methanol) [5] , 2%  
 Microscopy) SEM(Scanning Electron  
 Cr  
 TEM(Transmission Electron Microscope, JEOL JSM-2000FX) EDX(Oxford Link ISIS-  
 5947) carbon  
 extraction replica [5] , Cr  
 80 $\mu$ m polishing , 3mm disk 60%  
 methanol+36% bothylcellosolve+4%perchloric acid DC 20V, 45~55mA  
 jet polishing

### 2.3

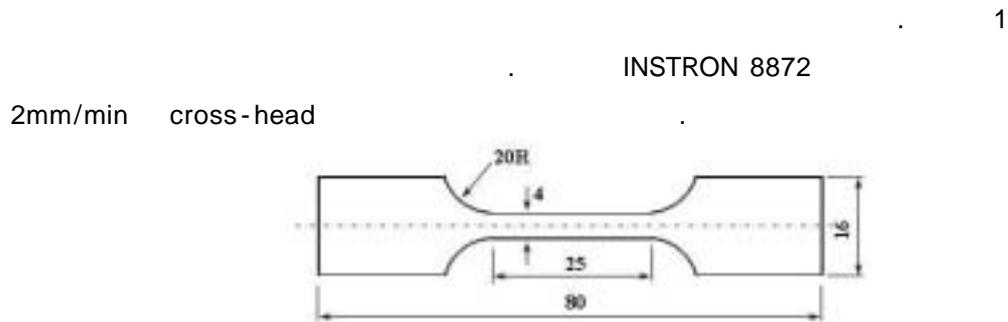


Fig. 1 Shape and dimensions of tensile specimens. (unit: mm)

### 2.4

SCC U-bend ( 2). 2(a) 가 ,  
 2(b) U- , polishing  
 , 가 가 , U-  
 bend (total strain, ) [6].

$$\sigma = T/2R \quad (T \text{ R } )$$

, T , R U-bend U-bend  
 7.9% .  
 SCC 2 U-bend , 315 , 40% NaOH  
 2 Ni 200 autoclave . U-bend 40% NaOH

autoclave , 1  
 , cover gas 5% $H_2$ -95% $N_2$  가 200psi 가 .  
 U-bend 가 ,  
 EG&G model 363 potentiostat/galvanostat  
 200mV 가 , Ni wire (reference electrode) ,  
 autoclave (count electrode) [4,7-8].  
 가 , 60 .

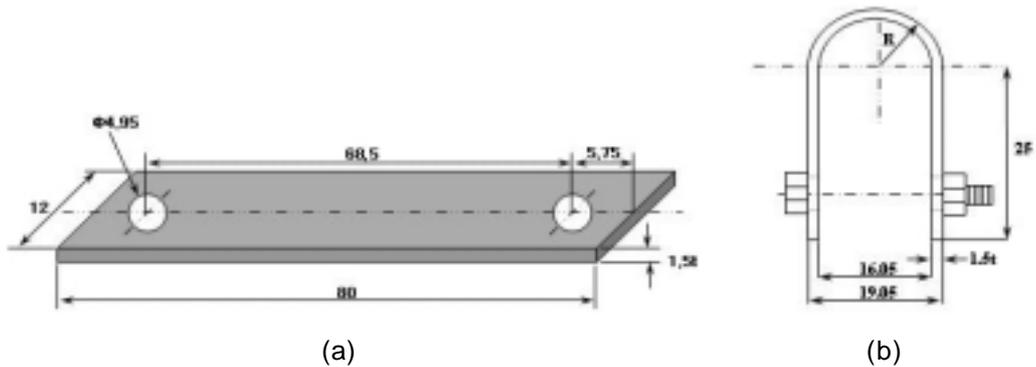


Fig. 2 Dimensions of rectangular strip and stressed U-bended specimens: (a) rectangular and (b) stressed U-bend. (unit : mm)

### 3.

#### 3.1

##### 3.1.1

900~1100 30 SA . 3 SA ,  
 , Ce 가 600CE4가 600CE0 .  
 600CE4 가 Ce . Wang[9,10] laser clad  
 coating Ce 가가 . Ce  
 (rare earth)  
 가 . O S  
 , 가 ,  
 가 [9].  
 , Ce 1.83 , 1.25 Fe, 1.24 Cr Ni  
 , Ce가 가 가 ,  
 Ce가  
 [9,11]. Ce  
 Ce dragging effect

[9]. , 600CE4  
600CE0

가 Ce

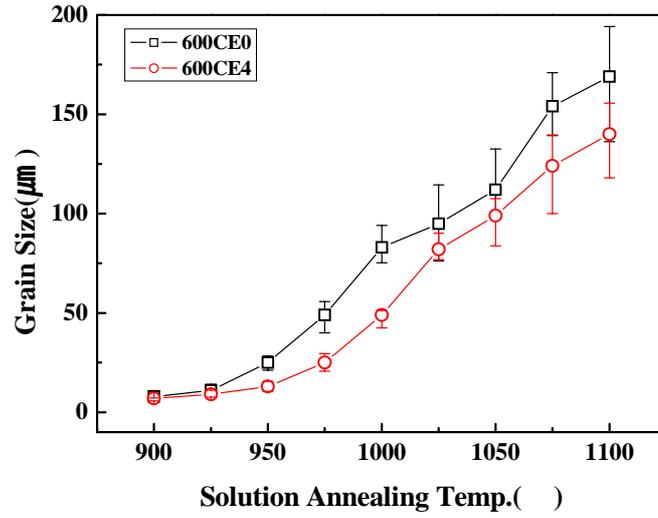


Fig. 3 Temperature dependence of grain size of the model alloys after solution annealing treatment.

가 SCC  
가 32μm [12], 가 35μm 가  
3 SA 가 SA  
600CE0 975 20 , 600CE4 1010 10 ,  
4

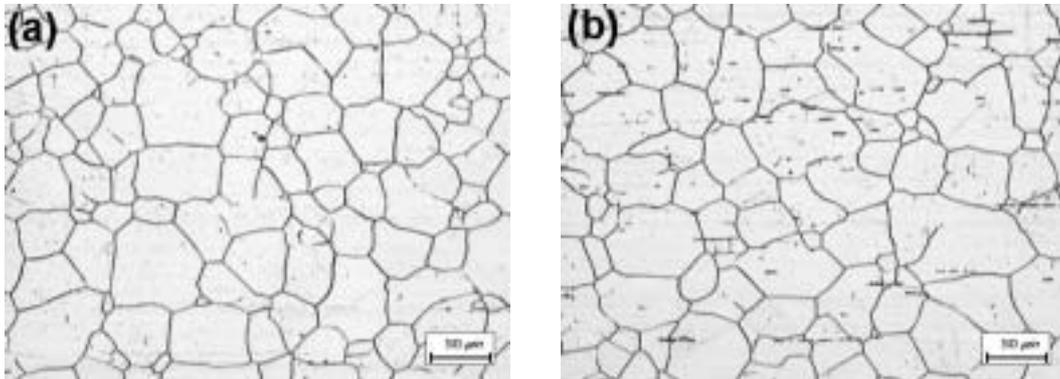


Fig. 4 Optical micrographs of model alloy 600 samples after solution annealing: (a) 600CE0 at 975°C for 20min, (b) 600CE4 at 1010°C for 10min.

### 3.1.2

Alloy 600 SCC  
(semicontinuous) 가  
[2,3]. ,  
, SA TT Ce  
가 SA 600CE0 600CE4 704 2~96

TT

4 5

4

SEM

4(a), (e)

TT

TT

가

가 가

, TT

600CE0가 600CE4

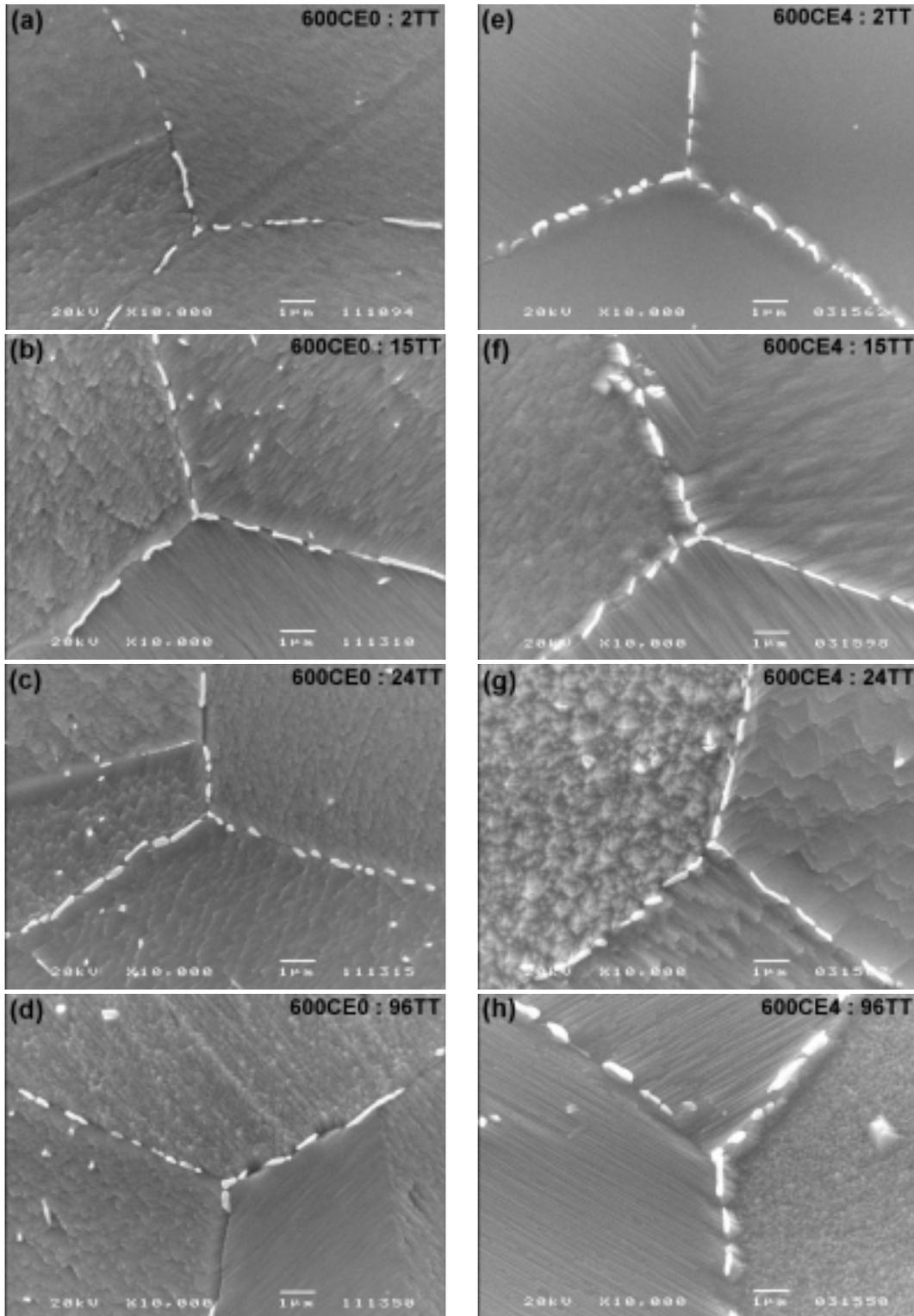
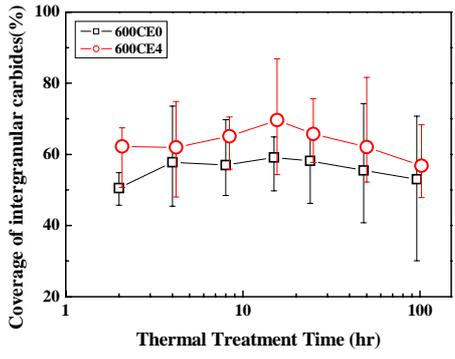


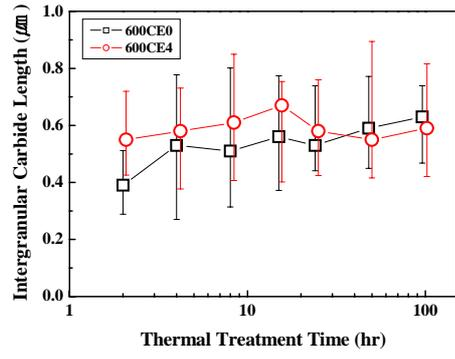
Fig. 4 SEM micrographs showing grain boundary carbides in 600CE0 after thermal treatment at 704 °C for (a) 2hr, (b) 15hr, (c) 24hr, (d) 96hr and 600CE4 after thermal treatment at 704 °C for (e) 2hr, (f) 15hr, (g) 24hr, (h) 96hr.

가 600CE0 TT 5 (a) 가 15 15 600CE4가 10% 0.67 $\mu$ m 0.56 $\mu$ m 600CE0 0.11 $\mu$ m TT 600CE4 24 가 TT 가 가

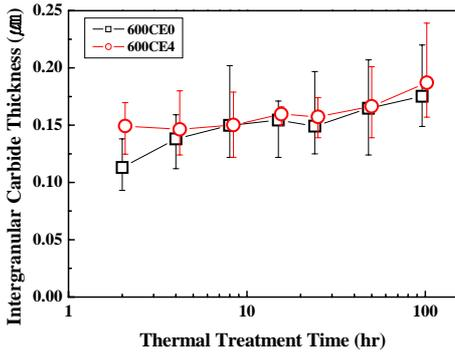
가 Ce 가 600CE4 가 600CE0 가



(a) carbide coverage



(b) carbide length



(c) carbide thickness

Fig. 5 Variations of intergranular carbide size and distribution precipitated in the model alloys with thermal treatment time.

Ce

Ce Watanabe[11] site

TEM EDX TT , pseudo hexagonal  $Cr_7C_3$  , FCC  $Cr_{23}C_7$

[13], Alloy 600 Ce 가

704 15 TT carbon extraction replica [5]

6(a) (c) EDX TEM , TEM

6(b) (d) 98.4 wt% Cr, 1.6 wt% Fe 6(a)

600CE0 EDX , (streak)가

6(b) ,  $Cr_7C_3$  (stacking fault energy)

[14].

$Cr_7C_3$  6(c) (d) 600CE4

96.9wt% Cr, 2.0wt% Fe, 1.2wt% Ni  $Cr_7C_3$

Ce

Ce 가 Ce EDX

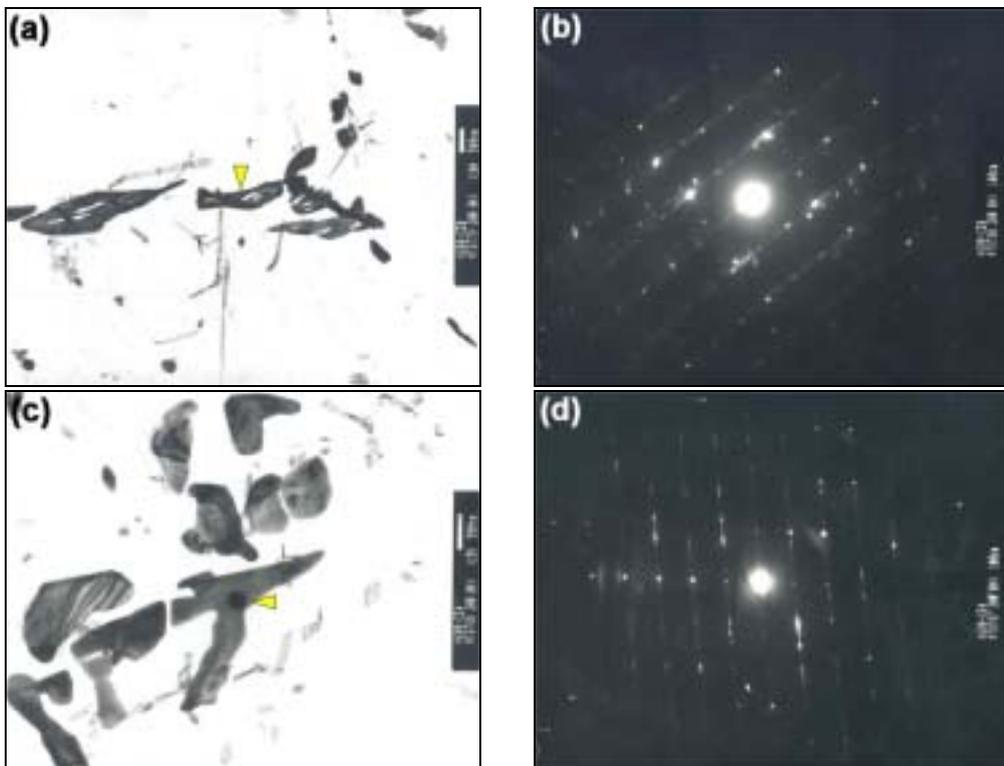


Fig. 6 TEM micrographs and selected area diffraction pattern of the carbide precipitates of model alloy 600 after thermal treatment at 715 for 15hr for (a), (b)600CE0 and (c), (d) 600CE4.

### 3.1.3

Cr 가 Cr 가  
 . Ce가 Cr  
 SA 704 15 TT 600CE0 600CE4 Cr  
 TEM EDX . Ce TEM EDX  
 200nm 가 Cr TEM  
 7 , 8 Cr Cr  
 17 wt% , Cr 600CE0 12.4 wt%, 600CE4 11.9 wt% ,  
 600CE4가 Cr  
 가 . Cr , 300nm . ,  
 Ce , Ce 가

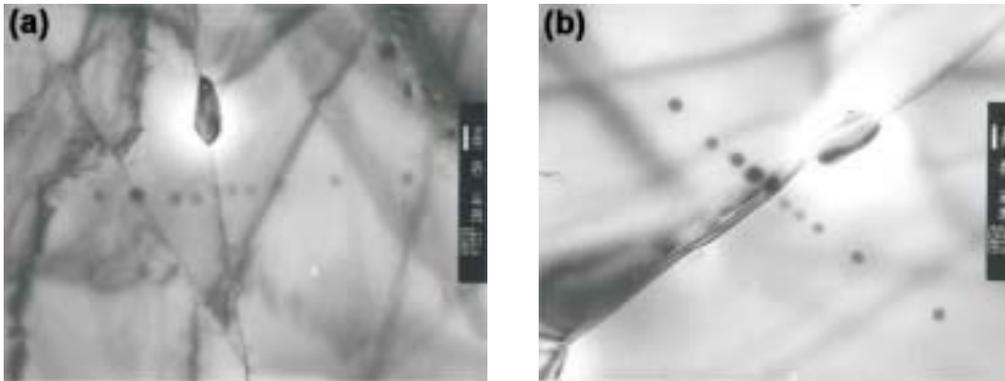


Fig. 7 TEM electro beam trace across a grain boundary and between carbides of alloys of (a) 600CE0 and (b) 600CE4 after thermal treatment at 704 for 15hr

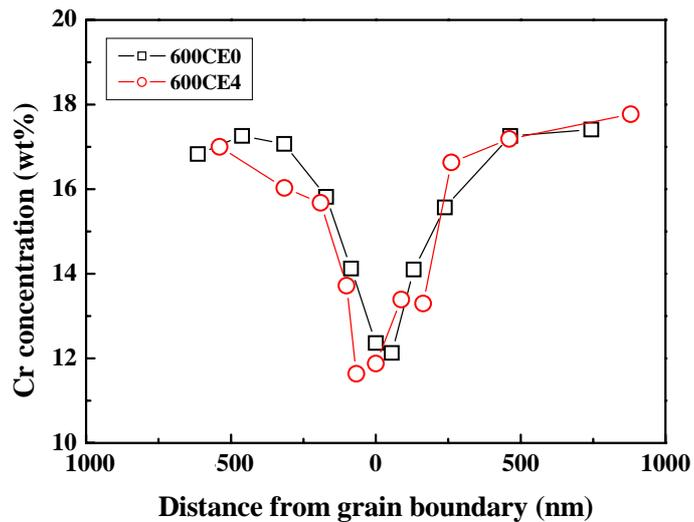


Fig 8. Cr concentration profiles around grain boundaries of the model alloys after thermal treatment at 704 for 15hr.

### 3.2

가 , SA 704 15 TT  
 9  
 2 9  
 9 2 0.2% (0.2% offset yield strength),  
 (ultimate tensile strength) (elongation)  
 , Ce가 600

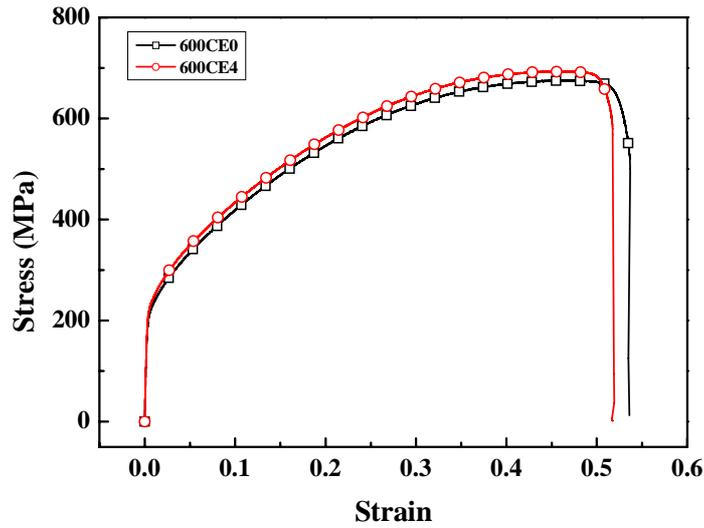


Fig. 9 Stress-Strain curves of model alloy specimens determined in air at room temperature.

Table 2 Mechanical properties of model alloy 600.

	0.2% offset YS(MPa)	UTS(MPa)	Elongation (%)
600CE0	212	677	40.4(±1.2)
600CE4	219	694	40.6(±0.2)

### 3.3

SA 704 15 TT U-bend  
 315 , 40% NaOH autoclave 200mV 가 60 SCC  
 , U-bend 3  
 10  
 11  
 11 4 600CE0 1279μm ,  
 600CE4 946μm 600CE4가 600CE0 SCC

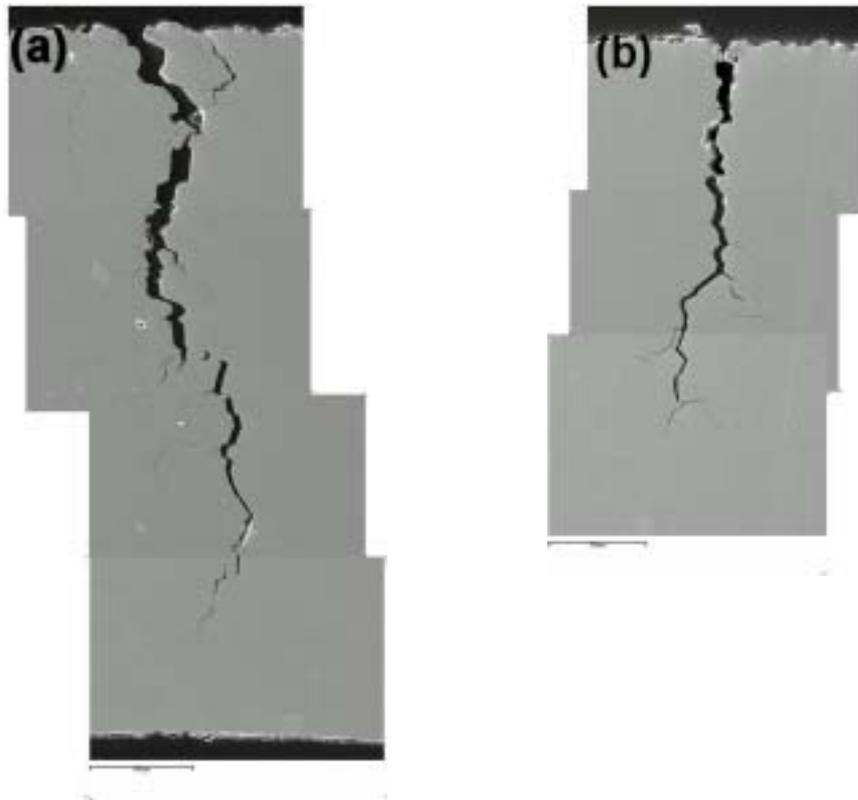


Fig. 10 SEM micrographs of cracks occurring in U-bend specimens tested in 40% NaOH solution at 315 for 60hr: (a) 600CE0 and (b) 600CE4.

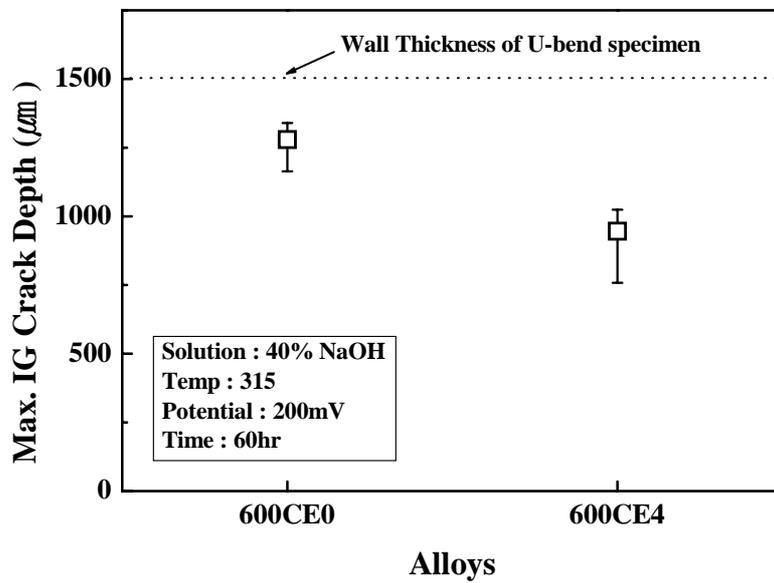


Fig. 11 Maximum IG crack depth of U-bend specimens tested in 40% NaOH solution at 315 for 60hr.

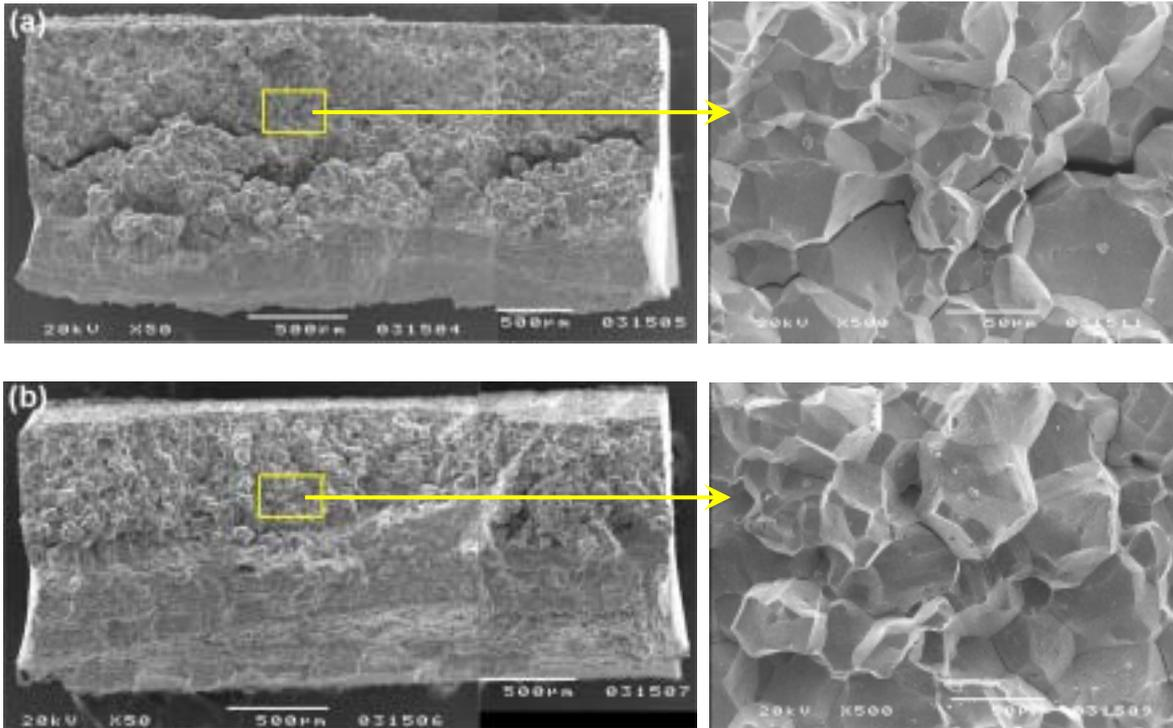


Fig. 12 SEM micrographs of fracture surfaces on the tested specimens in 40% NaOH solution at 315 °C for 60hr: (a) 600CE0 and (b) 600CE4.

4.

SCC  
 Ni, Cr Fe , Ce 가 , SA  
 . TT autoclave SCC ,  
 , U-bend  
 SCC  
 가 Ce .  
 , SCC Ce 가 600CE4가  
 SCC  
 600CE0 600CE4 pseudo hexagonal Cr<sub>7</sub>C<sub>3</sub> ,  
 Cr Cr 가 . 600CE4가 ,  
 가 TT 가 , TT  
 600CE4 . 가가 SCC  
 [15,16], Ce 가  
 SCC 가 Ce 가 .  
 600CE4 Ce Ce  
 가 .

## 5.

Ce 가 Ce 가 ,  
SCC Ce

- 1) pseudo hexagonal Cr<sub>7</sub>C<sub>3</sub> , Cr  
Cr Ce 가
- 2) Ce 가 ,
- 3) Ce 가 SCC ,

## 6.

- [1] J. B. Lumsden, P. J. Stocker, *Proc. Forth Int. Symp. on Environmental Degradation of Materials in Nuclear Power Systems - Water Reactors*, pp. 6-38 (1991)
- [2] Ph. Berge, J. R. Donati, B. Prioux and D. Villard, *Corrosion*, **Vol. 33**, p. 425 (1977)
- [3] J. R. Crum, *Corrosion*, **Vol. 38**, pp.40-45 (1982)
- [4] D. H. Hur, J. S. Kim, J. S. Baek and J. G. Kim, *Corrosion*, **Vol. 58**, No. 12, pp. 1031-1038 (2002)
- [5] Y. S. Lim, "A study on the microstructure and corrosion characteristics of laser surface melted Ni-base Alloy 600", Ph.D. Thesis, KAIST, (2000)
- [6] ASTM standard E 112-88, "Standard practice for making and using U-bend stress-corrosion test specimens", (1985).
- [7] N. Pessall, *Corrosion Science*, **20**, pp. 225-242 (1980)
- [8] J. R. Cels, *Corrosion*, **Vol. 34**, p.198 (1978)
- [9] K. L. Wang, Q. B. Zhang, M. L. Sun, X. G. Wei and Y. M. Zhu, *Corrosion Science*, **43**, p. 255 (2001).
- [10] K.L. Wang, Y. M. Zhu, Q. B. Zhang and M. L. Sun, *Journal of Material Processing Technology*, **63**, pp.563-567 (1997)
- [11] Y. Watanabe, V. Kain, T. Tonozuka, T. Shoji, T. Kondo and F. Masuyama, *Scripta mater.*, **42**, pp. 307-312 (2000).
- [12] Combustion Eng. Specification No. 00000-MCM-063, Rev. 02
- [13] D. R. Johns and F. R. Beckiti, *Corrosion Science*, **30** (213), pp. 223-237 (1990).
- [14] D. J. Dyson and K. W. Andrews, *L. Iron Steel Inst.*, **Vol. 207**, pp. 208-219 (1969).
- [15] D. C. Crawford and G. S. Was, *Met. Trans. A*, **Vol. 23A**, No. 4, p. 1195 (1992)
- [16] G. J. Theus, et al., *EPRI NP-3061*, (1983)